An optical study of the D–D neutron irradiation-induced defects in Co- and Cu-doped ZnO wafers*

Wang Yun-Bo(王云波), Li Gong-Ping(李公平)†, Xu Nan-Nan(许楠楠), and Pan Xiao-Dong(潘小东)

School of Nuclear Science and Technology, Lanzhou University, Lanzhou 730000, *China*

(Received 18 June 2012; revised manuscript received 19 September 2012)

Room-temperature photoluminescence and optical transmittance spectroscopy of Co-doped (1×10^{14}, 5×10^{16}, and 1×10^{17} cm^{-2}) and Cu-doped (5×10^{16} cm^{-2}) ZnO wafers irradiated by D–D neutrons (fluence of 2.9×10^{10} cm^{-2}) have been investigated. After irradiation, the Co or Cu metal and oxide clusters in doped ZnO wafers are dissolved, and the würtzite structure of ZnO substrate for each sample remains unchanged and keeps in high *c*-axis preferential orientation. The degree of irradiation-induced crystal disorder reflected from the absorption band tail parameter (E_0) is far greater for doped ZnO than the undoped one. Under the same doping concentration, the Cu-doped ZnO wafer has much higher irradiation-induced disorder than the Co-doped one. Photoluminescence measurements indicate that the introduction rate of both the zinc vacancy and the zinc interstitial is much higher for the doped ZnO wafer with a high doping level than the undoped one. In addition, both crystal lattice distortion and defect complexes are suggested to be formed in doped ZnO wafers. Consequently, the Co- or Cu-doped ZnO wafer (especially with a high doping level) exhibits very low radiation hardness compared with the undoped one, and the Cu-doped ZnO wafer is much less radiation-hard than the Co-doped one.

Keywords: D–D neutron irradiation, ZnO wafer, Co, Cu

PACS: 61.80.Hg, 61.82.Fk, 61.72.J–, 78.55.Et **DOI:** 10.1088/1674-1056/22/3/036102

1. Introduction

Diluted magnetic semiconductors (DMSs) produced by doping a small amount of transition metal (TM) ions into non-magnetic semiconductors have attracted intense interest as potential spintronic materials, and are expected to play an important role in opto- and magneto-electronics devices, which exploit spin in magnetic materials along with the charge of electrons in semiconductors.[1] After the theoretical prediction that p-type ZnO doped with Mn would show above-room-temperature ferromagnetism was made by Dietl *et al*.,[2] a great deal of research efforts have been focused on searching for room-temperature ferromagnetism in TM-doped ZnO systems. The observation of room-temperature ferromagnetic behavior in Co- or Cu-doped ZnO systems prepared by various methods (such as ion implantation, magnetron co-sputtering, and pulsed-laser deposition) have been reported by many groups.[3–9] In our group, the room-temperature ferromagnetic behavior was also observed in Co- and Cu-doped ZnO wafers prepared by ion implantation technique, and the microstructure of Co-doped ZnO was investigated in detail by means of the extended X-ray absorption fine structure (EXAFS) and X-ray photoelectron spectroscopy (XPS).[10–12] In order to understand and characterize the defects in ZnO semiconductors which have an important effect on the electronic and optoelectronic properties of semiconductor materials, a variety of experiment methods (i.e., positron annihilation lifetime spectroscopy (PALS), electron paramagnetic resonance (EPR), and cathodoluminescence (CL)) have been used for the investigation of the nominally pure ZnO semiconductors irradiated by high-energy electrons, protons, heavy ions, and fast neutrons from a reactor.[13–19] These investigations have provided detailed information about ZnO defects from different aspects, and proved that ZnO is more resistant to radiation damage than other common semiconductor materials (such as Si, GaAs, and GaN),[14,15] and thus potentially useful for applications in high-irradiation environments. However, the radiation effects of TM-doped ZnO systems have been rarely reported in literatures. Recently, Kumar *et al*.[6] reported a study aimed at shedding some light on the origin of ferromagnetism in Co-doped ZnO systems; they found that after 200-MeV Ag^{+15} ion irradiation, the Co-doped ZnO thin films exhibited room-temperature ferromagnetic behavior, the Co clusters in Co-doped ZnO were dissolved, and single-phase Co-substituted ZnO was formed. Dinia *et al*.[4] reported that after 40-keV He ion irradiation, the magnetic moment per Co in $Zn_{0.75}Co_{0.25}O$ thin film was increased, and the crystalline quality was improved. These findings are just about the heavy ions-irradiation influence on the ferromagnetism of Co-doped ZnO. However, the systematic investigation of high-energy particle irradiation-induced structural damage in Co- or Cu-doped ZnO systems is lacking.

In this work, due to both an excellent ability to pene-

*Project supported by the Key Laboratory for Magnetism and Magnetic Materials of the Ministry of Education at Lanzhou University of China (Grant No. LZUMMM2012003), the Chunhui Project of the Ministry of Education of China (Grant No. Z2008-1-62023), and the Fundamental Research Funds for the Central Universities of Ministry of Education of China (Grant No. 860452).

†Corresponding author. E-mail: ligp@lzu.edu.cn

© 2013 Chinese Physical Society and IOP Publishing Ltd

trate materials and a good monochromaticity of D–D neutrons (2.5 MeV), we attempt to experimentally investigate the D–D neutron irradiation-induced defects in Co- and Cu-doped ZnO wafers at room temperature by using X-ray diffraction (XRD), ultraviolet (UV)–visible absorption spectroscopy, and room-temperature photoluminescence (PL) measurements. Changes in the structural and optical properties of Co- and Cu-doped ZnO wafers induced by D–D neutron irradiation are discussed. To some extent, this investigation is of significance both for the understanding of the Co- and Cu-doped ZnO semiconductors' resistance to radiation and for the application of Co- or Cu-doped ZnO in high-irradiation environments, because the irradiation-induced defects play an important role in the degradation of devices.

2. Experimental procedure

The nominally pure ZnO (001) single-crystal wafers used in our experiments, with dimensions of $10.0\times10.0\times0.5$ mm^3, were purchased from MaTecK GmbH (Germany) and grown by using the hydrothermal technique. The Co- and Cu-doped ZnO wafers were prepared by using the ion implantation technique.[10,11] The pure ZnO single-crystal substrates were implanted at room temperature with 80-keV Co^+ (70-keV Cu^+) ions to the fluences of 1×10^{14}, 5×10^{16}, and 1×10^{17} cm^{-2} (5×10^{16} cm^{-2}) into the (001) growth face, respectively. These doped wafers, which were subsequently annealed at 700 °C for 30 min in flowing argon gas and naturally cooled down to room temperature to recover the implantation damage, showed room-temperature ferromagnetism.

The undoped ZnO, Co-doped ZnO with fluences of 1×10^{14}, 5×10^{16}, and 1×10^{17} cm^{-2}, and Cu-doped ZnO with a fluence of 5×10^{16} cm^{-2} were labeled as sample A, B, C, D, and E, respectively. All samples with different sizes were stacked together (the order is E, B, C, D, and A) and wrapped in aluminum foil to prevent them from being contaminated during irradiation. The wafers were irradiated with D–D neutrons (2.5 MeV) to a fluence of 2.9×10^{10} cm^{-2}. The irradiation was performed on the ZF-300-II neutron generator of Lanzhou University at room temperature. All wafers were irradiated on the ZnO (001) growth face, and located at the position of 45° exiting angle of D–D neutrons with an average distance of 3.2 cm from the center of the target chamber in the neutron generator (sample E was the closest to the target chamber). It is well known that as a neutral particle, the fast neutron has an excellent ability to penetrate materials. The total thickness of all our wafers is only 2.5 mm (0.5 mm for each). Therefore, the irradiation dose for each wafer can be considered to be approximately equal to one another. In order to study the damages caused by elastic or inelastic collisions of fast neutrons, we expect that the total concentration of the impurities transmuted in our samples is very low and negligible. According to information from the National Nuclear Date Center (NNDC), the 2.5-MeV neutron-activation cross sections of the eleven primary isotopes (^{64}Zn, ^{66}Zn, ^{67}Zn, ^{68}Zn, ^{70}Zn, ^{16}O, ^{17}O, ^{18}O, ^{59}Co, ^{63}Cu, and ^{65}Cu) existing in our samples are very low and negligible. Furthermore, after irradiation we measured the neutron-irradiated samples at room temperature using a NaI(Tl) detector as early as possible, and found no obvious radioactivity.

The structural characterizations of Co-, Cu-doped, and undoped ZnO wafers were carried out by X-ray diffraction (XRD) using a Rigaku D/Max-2400 diffractometer with a CuK_α ($\lambda = 1.54056$ Å) radiation source. In order to understand the defects introduced in samples, the optical transmittance spectra were recorded using a PGeneral TU-1901 UV spectrophotometer in the range of 300–900 nm at room temperature. Room-temperature photoluminescence (PL) measurements were performed under the excitation of a He–Cd laser (325 nm) using a Shimadzu RF-510 spectrophotometer.

3. Results and discussion

Figure 1 shows the X-ray diffraction θ–2θ scans of Co-, Cu-doped, and undoped ZnO wafers before and after D–D neutron irradiation. Samples A, B, C, D, and E are undoped, Co-doped (1×10^{14}, 5×10^{16}, and 1×10^{17} cm^{-2}), and Cu-doped (5×10^{16} cm^{-2}) ZnO wafers, respectively. Obviously, the rocking curve of each unirradiated or neutron-irradiated samples shows two very strong reflection peaks, which correspond to the characteristic (002) and (004) directions of the hexagonal würtzite-structure ZnO, respectively. This indicates that after irradiation the ZnO würtzite structure of each sample is not changed and keeps in high c-axis preferential orientation. Compared with the undoped ZnO wafer, the (002) diffraction peak position is located at a higher angle in each unirradiated/neutron-irradiated doped one. This is consistent with the fact that the effective ionic radius of Zn^{2+} (0.60 Å) is slightly larger than that of Co^{2+} (0.58 Å) or Cu^{2+} (0.57 Å) in tetrahedral coordination,[5,8] which implies that the Co^{2+} or Cu^{2+} ions substitute for Zn^{2+} in the ZnO lattice before and after irradiation. It is also found that after irradiation the (002) peak position slightly shifts leftward in each Co-doped ZnO wafer and rightward in Cu-doped ZnO wafer (no shift in undoped ZnO), as compared with the unirradiated one, respectively. This is probably because the amount of Co^{2+}/Cu^{2+} ions substituting for Zn^{2+} in doped ZnO wafer is decreased/increased due to D–D neutrons bombardment. In addition, after irradiation the full width at half maximum (FWHM) of the (002) reflection increases slightly for undoped and Cu-doped ZnO wafers, suggesting a small decrease of their crystalline quality. However, they all still have good single-crystal quality because of their low values

of FWHM equal to 0.32° and 0.24°, respectively. There is no significant change in the (002) peak FWHM of each Co-doped ZnO wafer.

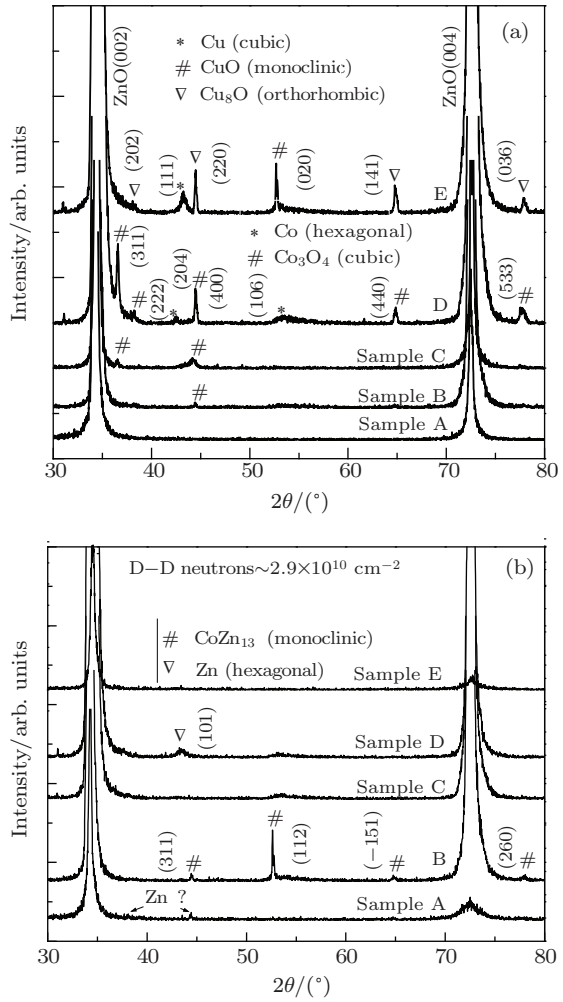


Fig. 1. X-ray diffraction $\theta - 2\theta$ scans for all wafers (a) before and (b) after irradiation. Samples A, B, C, D, and E stand for undoped ZnO, Co-doped ZnO with fluences of 1×10^{14}, 5×10^{16}, and 1×10^{17} cm^{-2}, and Cu-doped ZnO with a fluence of 5×10^{16} cm^{-2}, respectively.

In Fig. 1(a), the weak diffraction peaks from precipitate phases identified as crystalline Co, Co_3O_4, Cu, CuO, and Cu_8O clusters can be clearly observed on the Co- and Cu-doped ZnO wafers. Note that their intensities are far lower than those of the (002) and (004) peaks, and increase with increasing Co concentration in Co-doped ZnO wafers. Figure 1(b) shows the absence of these peaks, which indicates that the Co- or Cu-related clusters in unirradiated Co- or Cu-doped ZnO are dissolved after neutron irradiation. Interestingly, after irradiation the weak diffraction peaks from the secondary phase we identify as monoclinic $CoZn_{13}$ and hexagonal Zn appear in samples B and D, respectively, while there is no peak from the secondary phase in samples C and E. The (101) direction of the hexagonal Zn structure was also reported in Ref. [18]. This fact suggests that the Zn ions may be knocked out from the lattice into interstitial sites, and agglomeration of interstitial Zn and Co ions probably leads to the formation of $CoZn_{13}$ or Zn clusters. The formation of stable Zn-related clusters may be related to the dopant concentration in ZnO matrixes because their formation appears only in Co-doped ZnO wafers at 1×10^{14} and 1×10^{17} cm^{-2}, but not in Co- and Cu-doped ZnO wafers at 5×10^{16} cm^{-2}. Two very weak peaks observed on the neutron-irradiated undoped ZnO are possibly from the hexagonal zinc clusters, but their positions are slightly different from the corresponding peaks of the hexagonal zinc crystal reported in Ref. [18]. The above results imply that after D–D neutron irradiation the Co/Cu metallic and oxide clusters present in doped ZnO wafers are dissolved, and a small amount of $CoZn_{13}$ and Zn clusters are formed in Co-doped ZnO wafers 1×10^{14} and 1×10^{17} cm^{-2}, resepectively.

Figure 2 shows the room-temperature optical transmittance spectra of all wafers before and after neutron irradiation. It is evident that before irradiation, a weak absorption edge centering around 658 nm (1.88 eV) exists in samples C and D, respectively, and an absorption edge at around 600 nm (2.07 eV) in sample E. The 658-nm characteristic absorption edge is due to the d–d transitions in tetrahedrally coordinated high-spin Co^{2+} ($3d^7$) ions substituting Zn^{2+}, and attributed to the $^4A_2(F) \rightarrow {}^2E(G)$.[3] Generally, three characteristic absorption bands that are separately derived from $^4A_2(F) \rightarrow {}^2E(G)$, $^4A_2(F) \rightarrow {}^2T_1(P)$, and $^4A_2(F) \rightarrow {}^2A_1(G)$ transitions of tetrahedrally coordinated Co^{2+} can be observed on the Co-doped ZnO thin films.[3,7] However, only one absorption band can be observed in our Co-doped ZnO wafers. One possible reason is that two other absorption bands may be not strong enough in our samples. Since the thickness of each wafer (0.5 mm) is much greater than that of thin film, the transmittance of visible light in ZnO wafers is very low compared with thin films, which probably makes them unable to obviously display on transmittance spectra. The absence of 658-nm absorption edges in sample B may imply that the amount of Co^{2+} ions in tetrahedral sites is too low to be detected on the transmittance spectrum. After irradiation, the 658-nm absorption edge disappears in samples C and D, respectively, which suggests that the Co^{2+} ions substituting Zn^{2+} are probably displaced from their lattice sites due to D–D neutron bombardment. The 600-nm characteristic absorption edge on the unirradiated Cu-doped ZnO has been mainly thought to be due to the Cu surface plasmon resonance from copper metallic clusters.[21] The absence of 600-nm absorption in neutron-irradiated Cu-doped ZnO suggests that the copper clusters are dissolved after irradiation. The above results are consistent with the results of XRD. In addition, the transmittance of each doped ZnO wafer reduces sharply in the short-wavelength region (< 500 nm) after irradiation, which is due to the irradiation-induced defects.

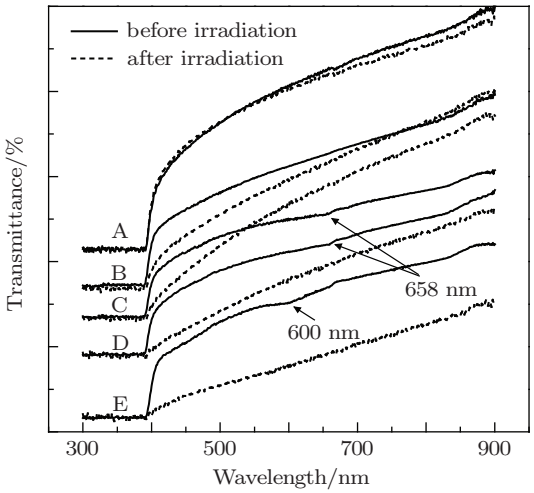


Fig. 2. Optical transmittance spectra at room temperature for the irradiated undoped, Co-, and Cu-doped ZnO wafers. The results for unirradiated ones are shown for comparison. The fluence of D–D neutron irradiation is 2.9×10^{10} cm^{-2}.

The optical band gap (E_g) of our samples can be estimated according to the following well-known expression for direct transition:[22]

$$\alpha E = A(E - E_g)^{1/2}, \quad (1)$$

where $E = h\nu$ is the photon energy, with h and ν being the Planck constant and the photon frequency, respectively, A is a constant, and α is the absorption coefficient. The α can be approximately calculated as:[7,23] $\alpha = -(1/D)\ln(T)$, where D and T are the thickness and transmittance of each wafer, respectively. Standard extrapolation of the linear portions of the curves to $(\alpha h\nu)^2 = 0$ ($E = E_g$) is plotted for the selected samples in Fig. 3. The estimated E_g values of all samples are listed in Table 1. It can be clearly seen that the E_g value of each unirradiated/neutron-irradiated Co- or Cu-doped ZnO wafer is lower (red-shift) than that of undoped ZnO which is not changed after irradiation. The red shift of the band gap has been ascribed to the sp–d exchange interactions between the band electrons and the localized d electrons of the Co^{2+}/Cu^{2+} ions in lattice sites.[9,24] The exchange interactions give rise to a negative and a positive correction to the energy of the conduction and valence bands, respectively, and lead to band-gap narrowing. From Table 1, it is also noticeable that for the Co-doped ZnO wafers the band gap slightly increases with increasing Co concentration, in contrast to that reported in Refs. [7] and [22]. This seems to mean that the amount of Co^{2+} ions substituting Zn^{+2} in Co-doped ZnO wafer at 1×10^{14} cm^{-2} is probably higher than that in Co-doped ZnO wafer at 5×10^{16} or 1×10^{17} cm^{-2}. Nevertheless, the analysis from Fig. 2 suggests that the amount of Co^{2+} should be higher in Co-doped ZnO wafers at 5×10^{16} and 1×10^{17} cm^{-2}. Additionally, the XRD results indicate that Co and Co_3O_4 clusters obviously exist in the Co-doped ZnO wafer at 5×10^{16} or 1×10^{17} cm^{-2}, and the diffraction peak from Co_3O_4 clusters in the Co-doped ZnO wafer at 1×10^{14} cm^{-2} is too weak and negligible. Based on these results, we conclude that the Co and/or Co_3O_4 clusters in Co-doped ZnO wafers probably have some influence on the absorption coefficient near the band edge, and cause the measured value of E_g to be larger than the actual value. After irradiation, the band gap increases in sample B, but decreased in samples C, D, and E. The increase of the band gap of Co-doped ZnO wafer at 1×10^{14} cm^{-2} may be due to the weakening of sp–d exchange interaction, indicating that the amount of Co^{2+} ions in ZnO lattice is reduced, which is in good agreement with the XRD result. The decrease of the band gap in Co-doped ZnO wafers at 5×10^{16} and 1×10^{17} cm^{-2} can be attributed to the dissolution of Co or Co_3O_4 clusters on the basis of the result shown in Fig. 1. As for the Cu-doped ZnO wafer, the decrease of band gap is also probably attributed to the dissolution of Cu-related clusters, whereas the contribution of enhancement of the sp–d exchange interaction (because after irradiation the number of Cu^{2+} ions substituting Zn^{2+} in Cu-doped ZnO wafer is increased (see Fig. 1)) is not excluded.

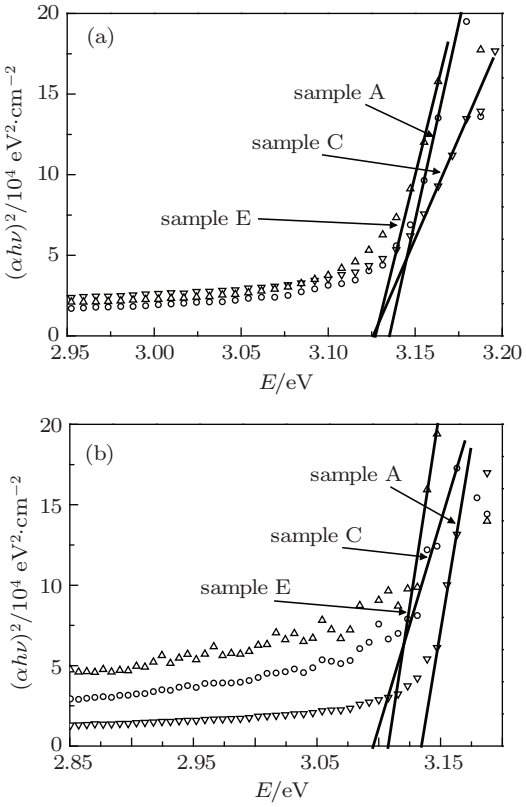


Fig. 3. Plots of $(\alpha h\nu)^2$ versus E for the undoped (sample A), Co-doped (sample C, 5×10^{16} cm^{-2}), and Cu-doped (sample E) ZnO wafers (a) before and (b) after irradiation. The fluence of D–D neutron radiation is 2.9×10^{10} cm^{-2}.

Table 1. Values of the band gap (E_g) and band tailing parameter (E_0) for the undoped, Co-, and Cu-doped ZnO wafers before and after D–D neutron irradiation.

Sample	E_g/eV		E_0/meV		ΔE_0/meV
	Before	After	Before	After	
Sample A	3.135	3.135	119.6	140.1	20.5
Sample B	3.120	3.129	237.2	367.1	129.9
Sample C	3.126	3.095	251.7	511.0	259.3
Sample D	3.131	3.062	225.6	526.8	301.2
Sample E	3.127	3.108	144.0	787.0	643.0

The effect of disorder caused by various defects (i.e., crystal distortion, point defects) in systems is highly pronounced in the lower energy tail of the sharp absorption edge. All possible defects (point, line, and planar defects) can lead to local electric fields that affect the band tailing.[25] Thus, to evaluate the neutron-induced defects in our samples using the band tailing effect, the relationship between $\ln(\alpha)$ and E (photon energy) for selected samples are shown in Fig. 4. The absorption coefficient $\alpha(E)$ in the near-band-edge region (band tailing) exponentially varies with photon energy as follows:[22]

$$\alpha(E) = \alpha_0 \exp(E/E_0), \tag{2}$$

where E is just below the band gap energy ($E < E_g$), α_0 is a constant, and E_0 is an empirical parameter with a dimension of energy describing the width of the localized states within the band gap. The value of E_0 can be determined from the reciprocal of the slope by fitting the linear part of the $\ln(\alpha)$–E curves, as shown in Fig. 4. Any defect or disorder in the crystal lattice can give rise to localized states within the band gap. Enhancement of E_0 indicates the increase of disorder in samples.[22,25] The obtained values of E_0, as well as the changes in E_0 (ΔE_0) with D–D neutron irradiation for all samples, are listed in Table 1. It can be clearly noted that for each sample, the value of E_0 increases after irradiation, and the magnitude of ΔE_0 is relatively large for doped ZnO wafers (largest for Cu-doped ZnO wafer) compared with the undoped one, and increases with the increasing Co doping concentration. Therefore, the degree of the irradiation-induced disorder reflected from the estimated value of ΔE_0 is the lowest and highest in the undoped and Cu-doped ZnO wafers, respectively, and increases with increasing Co concentration for Co-doped ZnO wafers. However, this observation is not consistent with the FWHM change of (002) peak in Fig. 1. A possible reason is that within the sensitivity of XRD, the effect of neutron irradiation-induced defects on the FWHM of (002) peak is not significant enough.

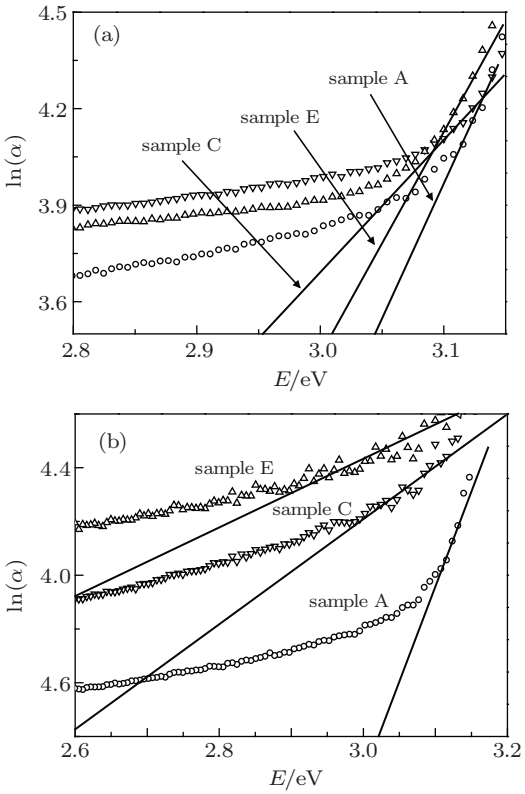


Fig. 4. Plots of $\ln(\alpha)$ versus E for the undoped (sample A), Co-doped (sample C, 5×10^{16} cm^{-2}), and Cu-doped (sample E) ZnO wafers (a) before and (b) after irradiation. The fluence of D–D neutron radiation is 2.9×10^{10} cm^{-2}.

The luminescence bands of ZnO usually consist of two parts, ultraviolet (UV) emission resulting from exciton recombination, and visible light (VL) emission from the structural defects related to deep-level emissions, such as zinc vacancy, oxygen vacancy, zinc interstitial, and oxygen interstitial.[20,26] Figure 5 shows the room-temperature PL spectra obtained from the undoped and Co-, Cu-doped ZnO wafers before and after neutron irradiation. It is interesting to note that before irradiation all samples show a typical luminescence behavior with the two emissions of narrow UV and broad green bands (the green emission on Cu-doped ZnO wafer is very weak and negligible), while after irradiation new emissions (violet emission) appear. In Fig. 5(a), the strong UV emissions at around 381.1, 382.7, 383.0, and 381.8 nm from the free-exciton recombination can be clearly observed on samples B, C, D, and E, respectively. They are all red-shifted in comparison with that (380 nm) of the undoped ZnO wafer. However, after irradiation the position of UV emission is shifted to 380 nm for sample B, 382.4 nm for sample E, and remains unchanged for sample A (see Fig. 3(b)). The UV emission peaks are all weakened for samples A, B, and E (very weak), and quenched for samples C and D. The variation of UV emission intensity is probably because a large number of nonradiative recombination centers, suppressing UV emission, are produced in samples.[17] Generally, the red-shift of UV emission can be interpreted as being due to exchange interactions (narrowing the band gap of ZnO) between band electrons and localized 3d electrons of Co^{2+}/Cu^{2+} ions substituting Zn^{2+}.[26] This implies that after irradiation the shift of the UV peak positions of samples B and C is due to the weakening and enhancement of sp–d exchange interaction, respectively, which suggests that the amount of Co^{2+}/Cu^{2+} ions substituting Zn^{2+} is decreased/increased, in good agreement with the results of XRD. Consequently, the Co interstitial ions and Zn vacancies (Frenkel pairs) may be generated because the Co^{2+} ions are knocked out from lattice to interstitial sites. In addition, before irradiation the shoulder emission centered at around 390 nm on the UV emitting band can be observed only on samples C and D. However, after irradiation this emission appears in each Co-doped ZnO wafer and increases in samples C and D, respectively, and no peak close to 390 nm appears in the undoped

ZnO wafer. This fact reveals that the emission at 390 nm may be attributed to the defects related to Co interstitial ions in Co-doped ZnO wafers. Liu *et al*.[27] reported that the emission at 393.8 nm on the UV emitting band was ascribed to bound exciton transition in $Zn_{1-x}Co_xO$ nanorod arrays, and the excitons were bound tightly by the defects including crystal lattice distortion, donors or acceptors introduced by Co dopant. We also note that an emission at 389 nm appears in the neutron-irradiated sample E (Cu-doped ZnO wafer at 5×10^{16} cm^{-2}), but no similar emission in the unirradiated one. Moreover, the degree of irradiation-induced disorder is very high in doped ZnO (highest in Cu-doped ZnO) compared with the undoped one (see Fig. 4). Accordingly, the crystal lattice distortion is possibly responsible for the 389- and 390-nm emissions in doped ZnO wafers because the probability of the formation of crystal distortion should be increased with the increase in the degree of irradiation-induced disorder. Based on the above results, we deduce that the 390-nm emission existing in Co-doped ZnO wafers is probably due to both the Co-related defects and crystal lattice distortion introduced by D–D neutron irradiation, and the 389-nm emission in Cu-doped ZnO is mainly due to the irradiation-induced crystal lattice distortion. Nevertheless, further investigation into this issue is needed.

It is also interesting to note that after irradiation the intensity of green emission is enhanced for sample A, but slightly reduced for sample B and strongly quenched for sample C and D. No significant or a very weak green emission can be observed in sample E before and after irradiation. It is generally accepted that the green emission is ascribed to the oxygen vacancy (V_O).[28,29] Therefore, the oxygen vacancies are introduced in undoped ZnO wafer due to D–D neutron bombardment. The irradiation-induced oxygen vacancies in nominally pure ZnO by high-energy electrons or fast neutrons have been abundantly reported.[13,16,18] The weakening or suppression of green emission is probably related to the nonradiative recombination centers introduced in neutron-irradiated Co-doped ZnO wafers.[17] Probably, both oxygen vacancies present in unirradiated Co-doped ZnO and irradiation-induced defects agglomerate to form defect complexes (i.e., V_{Zn}–Zn_O and V_{Zn}–Zn_O–O_{Zn}–Zn_i)[14,16,17] or vacancy clusters.[19] One should note that the degree of irradiation-induced disorder (ΔE_0) in each Co-doped ZnO wafer is much higher than that in the undoped one (see Table 1). Therefore, the probability of formation of defect complexes or vacancy clusters in Co-doped ZnO should be much larger than that in the undoped one (the Cu-doped ZnO wafer should have very large probability of introduction of defect complexes because of its highest value of ΔE_0 in all doped ZnO wafers).

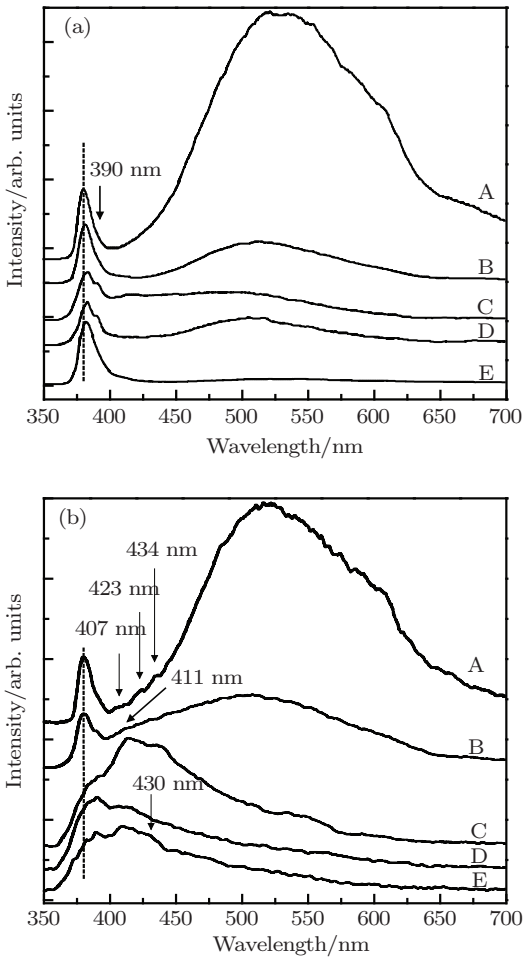


Fig. 5. Room-temperature PL spectra for the undoped, Co-, and Cu-doped ZnO wafers (a) before and (b) after irradiation. The fluence of D–D neutron radiation is 2.9×10^{10} cm^{-2}.

Additionally, after irradiation the violet emissions centering about 414 nm (2.99 eV) and 439 nm (2.82 eV) for sample C, 416 nm (2.98 eV) for sample D, and 410 nm (3.02 eV) and 430 nm (2.88 eV) for sample E can be clearly observed on Fig. 5(b). For sample B, a very weak shoulder peak of $\sim$ 411 nm (3.02 eV) on the green emitting band can be also observed. Three weak violet emissions at $\sim$ 407 nm (3.05 eV), 423 nm (2.93 eV) and 434 nm (2.86 eV) are on the green emitting band of sample A. Similar emissions have been reported. Mahamuni *et al*.[30] and Xu *et al*.[31] found the violet emission at 420 nm in ZnO quantum dots and thin films, respectively, and they all thought that this emission was attributed to the oxygen interstitial (O_i). However, Jin *et al*.[32] believed that the 420 nm emission was related to the interface trap in grain boundaries of ZnO films. For our samples, the 423 nm emission appeared only in undoped ZnO wafer and could not originate from the interface trap in the grain boundaries because after irradiation the undoped ZnO is still in good single-crystal quality (see Fig. 1) and its degree of irradiation-induced disorder is far lower than that in doped one (see Table 1). This emission is possibly attributed to the O_i. Here, the oxygen vacancies as reflected from the green emission are produced only

in undoped ZnO wafer after irradiation. This fact suggests that the oxygen interstitial sites resulting in 423 nm PL emission may be generated in undoped ZnO wafer due to Frenkel-pair formation. Jeong *et al.*[33] and Wu *et al.*[29] observed a violet emission at 401 nm and 405 nm in ZnO thin films, respectively, and all concluded that the Zn vacancy (V_{Zn}) was responsible for this emission. According to the theoretical energy levels of intrinsic defects in ZnO thin films calculated by full-potential linear muffin-tin orbital method,[34] the energy intervals both from the bottom of conduction band to V_{Zn} level and from the top of valence band to Zn_i level are 3.06 and 2.9 eV, respectively, which approach the energy of violet emissions appeared in our samples. In addition, it is very interesting to note that for our neutron-irradiated Co-doped ZnO wafers, the emission at 439 nm appears only in sample C and no emission close to 439 nm in the other wafers, while the X-ray diffraction peaks from Zn-related clusters merely appear in sample B and D. This means that the emission at 439 nm is probably due to the Zn_i. It should be also noted from Fig. 5(b) that the violet emission peak position approaching 400 nm shifts gradually from 407 nm to 416 nm when the Co doping concentration increases from 0 to 1×10^{17} cm^{-2}. This may be due to the fact that the band gap energies of neutron-irradiated samples are decreased with the increasing Co concentration, as shown in Table 1. Accordingly, the violet emission peaks at 407, 410, 411, 414, and 416 nm of our samples are all probably ascribed to the V_{Zn}, and the emission peaks at 430, 434, and 439 nm to the Zn_i. Based on these discussions above, we speculate from the violet emission intensities that by D–D neutron irradiation the total introduction rate of the defects of both V_{Zn} and Zn_i is observably high in (5×10^{16}, 1×10^{17} cm^{-2}) Co-doped ZnO or 5×10^{16} cm^{-2} Cu-doped ZnO wafer compared with the undoped one, which is consistent with the difference of degree of irradiation-induced disorder for all samples.

4. Conclusion

We have presented the experimental results obtained with XRD, PL, and optical transmittance spectroscopy for the D–D neutron-irradiated Co-, Cu-doped, and undoped ZnO wafers at room temperature. The cobalt or copper metal and oxide clusters existing in Co- and Cu-doped ZnO wafers were dissolved due to neutron bombardment. However, a small amount of $CoZn_{13}$ and Zn clusters were formed in Co-doped ZnO wafers at 1×10^{14} and 1×10^{17} cm^{-2}, respectively. The degree of irradiation-induced disorder, estimated from absorption band tail effect of transmittance spectra, is extremely high in each doped ZnO wafer (highest in the Cu-doped one) compared with the undoped one, and increases with the increase in Co concentration. The investigation of room-temperature PL reveals that the defects of V_{Zn} and Zn_i are introduced in Co-doped ZnO (5×10^{16}, 1×10^{17} cm^{-2}) and Cu-doped ZnO (5×10^{16} cm^{-2}) at the total introduction rate much higher than the undoped one. In addition, the V_O is introduced only in the undoped ZnO wafer, whereas those existing in the unirradiated Co-doped ZnO wafers probably take part in the formation of the defect complexes or vacancy clusters. We also believe that neutron irradiation introduces the significant Co-related defects and/or crystal lattice distortion in doped ZnO wafers. Based on these analyses, we conclude that both the type and the total concentration of defects introduced in doped ZnO wafer (especially with high doping level) are more complex and higher than those in the undoped one due to D–D neutron irradiation. Therefore, at room temperature the Co- or Cu-doped ZnO wafer, especially with high doping level, is much less resistant to D–D neutron irradiation than the undoped one, and the radiation hardness of Cu-doped ZnO wafer is very low when compared with the Co-doped one with the same doping concentration.

Acknowledgements

We would like to thank the ZF-300-II Neutron Generator group at Lanzhou University for providing D–D neutrons.

References

[1] Ohno H 1998 *Science* **281** 951
[2] Dietl T, Ohno H, Matsukura F, Cibert J and Ferrand D 2000 *Science* **287** 1019
[3] Ramachandran S, Tiwari A and Narayan J 2004 *Appl. Phys. Lett.* **84** 5255
[4] Dinia A, Ayoub J P, Schmerber G, Beaurepaire E, Muller D and Grob J J 2004 *Phys. Lett. A* **333** 152
[5] Kolesnik S, Dabrowski B and Mais J 2004 *J. Appl. Phys.* **95** 2582
[6] Kumar R, Singh F, Angadi B, Choi J W, Choi W K, Jeong K, Song J H, Khan M W, Srivastava J P, Kumar A and Tandon R P 2006 *J. Appl. Phys.* **100** 113708
[7] Liu X C, Shi E W, Chen Z Z, Zhang H W, Song L X, Wang H and Yao S D 2006 *J. Cryst. Growth* **296** 135
[8] Herng T S, Lau S P, Yu S F, Yang H Y, Ji X H, Chen J S, Yasui N and Inaba H 2006 *J. Appl. Phys.* **99** 086101
[9] Chakraborti D, Narayan J and Prater J T 2007 *Appl. Phys. Lett.* **90** 062504
[10] Li T J, Li G P, Chen J S, Gao X X, Pan X D, Ma J P and Wang Y B 2010 *Sci. China-Phys. Mech. Astron.* **53** 1819
[11] Li T J, Li G P, Chen J S, Gao X X and Chen J S 2010 *Chin. Phys. Lett.* **27** 087501
[12] Gao X X, Li G P, Li T J, Pan X D, Hu F C, He B and Bao L M 2011 *Integr. Ferroelectr.* **128** 14
[13] Leutwein K and Schneider J 1971 *Z. Naturforsch. A* **26** 1236
[14] Look D C, Reynolds D C, Hemsky J W, Jones R L and Sizelove J R 1999 *Appl. Phys. Lett.* **75** 811
[15] Auret F D, Goodman S A, Hayes M, Legodi M J, Laarhoven H A and Look D C 2001 *Appl. Phys. Lett.* **79** 3074
[16] Tuomisto F, Saarinen K, Look D C and Farlow G C 2005 *Phys. Rev. B* **72** 085206
[17] Chen Z Q, Wang S J, Maekawa M, Kawasuso A, Naramoto H, Yuan X L and Sekiguchi T 2007 *Phys. Rev. B* **75** 245206
[18] Evans S M, Giles N C, Halliburton L E and Kappers L A 2008 *J. Appl. Phys.* **103** 043710

[19] Zubiaga A, Tuomisto F, Coleman V A and Jagadish C 2008 *Appl. Surf. Sci.* **255** 234
[20] Cho S, Ma J, Kim Y K, Sun Y, Wong J K L and Ketterson J B 1999 *Appl. Phys. Lett.* **75** 2761
[21] Karali T, Can N, Valberg L, Stepanov A L, Townsend P D, Buchal C, Ganeev R A, Ryasnyansky A I, Belik H G, Jessett M L and Ong C 2005 *Physica B* **363** 88
[22] Dutta S, Chattopadhyay S, Jana D, Banerjee A, Manik S, Pradhan S K, Sutradhar M and Sarkar A 2006 *J. Appl. Phys.* **100** 114328
[23] Srikant V and Clarke D R 1998 *J. Appl. Phys.* **83** 5447
[24] Kim K J and Park Y R 2002 *Appl. Phys. Lett.* **81** 1420
[25] Srikant V and Clarke D R 1997 *J. Appl. Phys.* **81** 6357
[26] Zhu H C, Iqba J, Xu H J and Yu D P 2008 *J. Chem. Phys.* **129** 124713
[27] Liu Y M, Fang Q Q, Wu M Z, Li Y, Lü Q R, Zhou J and Wang B M 2007 *J. Phys. D: Appl. Phys.* **40** 4592
[28] Vanheusden K, Warren W L, Seager C H, Tallant D R, Voigt J A and Gnade B E 1996 *J. Appl. Phys.* **79** 7983
[29] Wu X L, Siu G G, Fu C L and Ong H C 2001 *Appl. Phys. Lett.* **78** 2285
[30] Mahamuni S, Borgohain K, Bendre B S, Leppert V J and Risbud S H 1999 *J. Appl. Phys.* **85** 2861
[31] Xu X L, Lau S P, Chen J S, Chen G Y and Tay B K 2001 *J. Cryst. Growth* **223** 201
[32] Jin B J, Im S and Lee S Y 2000 *Thin Solid Films* **366** 107
[33] Jeong S H, Kim B S and Lee B T 2003 *Appl. Phys. Lett.* **82** 2625
[34] Lin B X, Fu Z X and Jia Y B 2001 *Appl. Phys. Lett.* **79** 943